Highly Active Crystalline Mesoporous TiO2 Films Coated onto Polycarbonate Substrates for Self-Cleaning Applications

4 AUTHORS, INCLUDING:

Adel A Ismail
Central Metallurgical Research and Develop…

**64** PUBLICATIONS **1,555** CITATIONS

Highly Active Crystalline Mesoporous TiO$_2$ Films Coated onto Polycarbonate Substrates for Self-Cleaning Applications

Razan Fateh,[†] Adel A. Ismail,*[,‡] Ralf Dillert,[†] and Detlef W. Bahnemann[†]

[†]Institut für Technische Chemie, Leibniz Universität Hannover, Callinstrasse 3, 30167 Hannover, Germany

[‡]Advanced Materials Department, Central Metallurgical R&D Institute (CMRDI), P. O. Box 87 Helwan, Cairo 11421, Egypt

ABSTRACT: SiO$_2$ film precoating is found to be very effective for the protection of polycarbonate (PC) as a typical example for heat-sensitive substrate materials, thus preventing its photodegradation under UV light. Subsequently, transparent photoactive mesoporous TiO$_2$ and Sachtleben Hombikat UV100 thin film coatings on SiO$_2$/PC have been developed for self-cleaning applications. The newly prepared photocatalysts films have been compared with either a film prepared from a commercial photocatalyst (Sachtleben Hombikat UV-100), SG-TiO$_2$, or Pilkington Glass Activ^{TM} by the determination of their photonic efficiencies for degradation of methylene blue and the photo-induced surface wettability. The efficiency of the photocatalytic reactions was found to be about three times higher in the case of the mesoporous TiO$_2$ films compared with films prepared from UV-100 or Pilkington Glass Activ^{TM}. This is the first report focusing on the synthesis of mesoporous TiO$_2$ films on polycarbonate substrates, and, to the best of our knowledge, the measured photonic efficiency of ζ = 0.078% for these *meso*-TiO$_2$ films on PC is among the highest ζ-values reported up to now even when using soda-lime glass substrates.
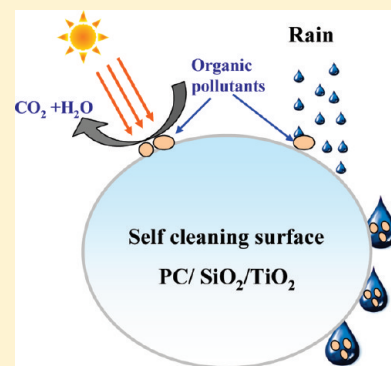
■ INTRODUCTION

Polycarbonate (PC) is a very durable material and can even be laminated to produce bullet-proof "glass", though "bullet-resistant" would be the more accurate description. PC replaces glass in many fields, especially in the automotive industry, because it is much softer and easily shapeable to comply with modern design requirements. Poor physical properties, such as low hardness and scratch resistance as well as poor photocorrosion resistance, pose a barrier for the adoption of PC for a wide range of industrial applications. Therefore, there is an urgent need to change or improve the properties at the surface of the polymer without altering its bulk properties.[1] PC is highly transparent to visible light exhibiting better light transmission characteristics than many types of silica glass. The problem is that PC has a glass transition temperature of about 150 °C and gradually softens above this point starting to flow above about 300 °C. To enable the use of polycarbonate in applications exposed to weathering or UV-radiation, a special surface treatment is needed. Several methods to apply TiO$_2$ coatings on various substrates have been developed promising to potentially exhibit highly interesting commercial applications such as self-cleaning, antibacterial properties, and waste remediation.[2] Compared with heat-proof substrates such as glass or steel, polymer substrates have a low surface energy and a high thermal sensitivity. To solve the thermal stability problem, different approaches have been proposed to prepare highly active photocatalytic TiO$_2$ films at low temperature. TiO$_2$ thin films on polyamide substrates have been prepared by magnetron sputtering.[3] However, the cost and the feasibility of the process are considerable. A sol−gel method has been used followed by the treatment of the films in boiling water

to prepare crystallized TiO$_2$ thin films exhibiting different properties depending upon the employed substrates.[4] Liquid phase deposition (LPD) was also applied to prepare TiO$_2$ films at low temperature exhibiting high photocatalytic activity.[5] However, the applicability of this approach appears to be limited due to its low depositing rate and the poor light transmittance of the resulting films. Some reports also describe the preparation of highly photocatalytcally active TiO$_2$ films on heat-sensitive substrates such as polystyrene, polycarbonate, poly(methyl methacrylate), and poly(ethylene terephthalate).[6−8]

Mesoporous TiO$_2$ has recently attracted much attention concerning its application as a photocatalyst to decompose environmental pollutants.[9−11] Nanosized TiO$_2$ particles usually show higher photocatalytic activities than the pigment type, because they have a larger surface area per unit mass and volume thus facilitating the diffusion of excited electrons and holes toward the surface before their recombination.[12] Among the different crystalline phases of TiO$_2$, anatase is reported to exhibit the highest photocatalytic activity.[13] Thus, the development of suitable techniques to form transparent anatase nanocomposite films on various substrates at low temperatures will be essential for practical applications of TiO$_2$ as a photocatalyst for pollutant-decomposition, for self-cleaning, and in hydrophilic surface systems.[14,15] In general, high uniformity of the mesoporous TiO$_2$ network regarding pore size, shape, and volume is known to be important for the improvement of the charge carrier transport processes.[16−18] And also, a large surface area, high

transmittance of ultraviolet (UV) light, and durability of the photocatalytic activity are required for the thin film in which anatase nanoparticles are dispersed without aggregation.[19]

Moreover, the coating of PC has to be achieved at low temperatures not exceeding 150 °C. For TiO_2 films prepared at low temperature, the crystallinity of the anatase phase is usually very weak and hence the associated photonic efficiencies are found to be very low.[4−8] Therefore, the present study is focused on the preparation of mesoporous TiO_2 with high uniformity and crystallinity, forming only one crystal phase (anatase) with small particle size and strong adsorptive capacity. For the PC substrate coating the newly prepared mesoporous TiO_2 has been dispersed into ethanol under vigorous stirring. The objective goals of this work were to investigate the photocatalytic and physical properties of the surface coatings on PC (Makrolon AL 2647) precoated with a layer of SiO_2 followed by the deposition of a layer of nanocrystalline mesoporous TiO_2. The newly prepared photocatalyst films have been compared with either commercial photocatalysts (Sachtleben Hombikat UV-100), SG-TiO_2, or with Pilkington Glass Activ™ by the determination of their photonic efficiencies for the degradation of methylene blue. The latter compound was used because it exhibits a high molar absorptivity (or molar extinction coefficient) allowing the rate of bleaching to be readily evaluated. This is the first report focusing on the synthesis of mesoporous TiO_2 films on PC substrates, and, to the best of our knowledge, the measured photonic efficiency of $\zeta = 0.078\%$ for these meso-TiO_2 films on PC is among the highest ζ-values reported up to now.

■ EXPERIMENTAL SECTION

Materials. The block copolymer surfactant EO_{106}-$PO_{70}EO_{106}$ (F-127, EO = $-CH_2CH_2O-$, PO = $-CH_2(CH_3)CHO-$), MW 12 600 g/mol), $Ti(OC(CH_3)_3)_4$ (TBOT), HCl, C_2H_5OH, and CH_3COOH were purchased from Sigma-Aldrich. Tetraethyl orthosilicate $Si(OC_2H_5)_4$ (TEOS) was provided by Roth. Commercial TiO_2 (Hombikat UV-100, 100% anatase) was kindly provided by Sachtleben Chemie GmbH. All chemicals were used as received.

Preparation of Coatings. *Preparation of SiO_2 Intermediate Layer.* The SiO_2 intermediate layer was prepared from (TEOS) via a sol−gel method to enhance the binding between the organic polymer and the inorganic layer and to protect the polycarbonate (PC, Makrolon AL 2647) from the photocatalytically active layer which may induce photodegradation of the PC. TEOS, ethanol, and deionized water were stirred for 30 min. Then hydrochloric acid was added into the mixture to catalyze the TEOS hydrolysis. The mixture was then stirred at ambient temperature for 24 h. The SiO_2 sol was deposited on the polycarbonate surface by dip-coating. The PC substrate slides were dipped into the SiO_2 solution and withdrawn into open air with a pulling rate of 1 mm/s one time. The produced films were dried at 80 °C for 24 h to evaporate the solvents and the HCl.

Synthesis of Mesoporous Titania. Mesoporous titania was prepared according to a procedure given in ref 20, which yields photocatalyst materials with a hexagonal mesostructure. Typically, 1.6 g of F127, 2.3 mL of CH_3COOH, and 0.74 mL of HCl were dissolved in 30 mL of ethanol and then added to 3.5 mL of TBOT. The mixture was stirred vigorously for 60 min. Ethanol was subsequently evaporated at 40 °C and a relative humidity of 40% for 12 h followed by the transfer of the sample into a 65 °C oven and aging for an additional 24 h. The as-made

mesostructured hybrids were calcined at 450 °C in air for 4 h to obtain hexagonal *P6m* mesoporous TiO_2 as has been shown in ref 20.

Synthesis of Titania Film on PC Substrates by Sol Gel-Methods (SG-TiO_2). PC slides precoated with SiO_2 were dipped in TiO_2 precursor. The coating was prepared via a sol−gel dip-coating method using titanium tetraisopropoxide as precursor for the TiO_2, Pluronic P123 as an organic template, and acidic ethanol as the solvent. The molar ratio of TIPT/P123/C_2H_5OH is 1:0.05:40. The pluronic was removed by solvent extraction using ethanol and hydrochloric acid. Then the films were dried at 80 °C in air for 24 h .The prepared films were used as-synthesized without calcinations and were denoted as SG-TiO_2.

Synthesis of Mesoporous Titania and Hombikat UV-100 Thin Films on PC Substrates. Mixtures of hydrochloric acid (0.1 N) and absolute ethanol were stirred at ambient temperature. Either mesoporous TiO_2 or commercial UV-100 (Sachtleben Hombikat) was added to the mixture with stirring. PC slides precoated with SiO_2 were dipped in the suspensions of meso-TiO_2 or UV-100 and subsequently withdrawn into the open air at a pulling rate of 1 mm/s three times. Then the film was aged at 80 °C in air for 24 h to evaporate the organic solvents and HCl.

Characterization. Transmission electron microscopy (TEM) was conducted at 200 kV with a JEOL JEM-2100F-UHR field-emission instrument equipped with a Gatan GIF 2001 energy filter and a 1k-CCD camera in order to obtain EEL spectra. Wide-angle X-ray diffraction (WXRD) data were acquired on a Bruker AXS D4 Endeavor X diffractometer using Cu $K\alpha_{1/2}$, $\lambda\alpha_1$ = 154.060 pm, $\lambda\alpha_2$ = 154.439 pm radiation, and small-angle X-ray diffraction (SXRD) patterns were recorded on a Bruker D8 Advance instrument. The nitrogen adsorption and desorption isotherms at 77 K were measured using a Quantachrome Autosorb 3B after the samples were vacuum-dried at 200 °C overnight. The sorption data were analyzed using the Barrett−Joyner−Halenda (BJH) model with the Halsey equation.[21] The surface relief of the mesoporous TiO_2 film was revealed by atomic force microscopy (AFM) using a digital instruments NanoScope apparatus. The absorption spectra of the films in the range 400−800 nm were recorded using a UV/vis spectrophotometer Cary 100Bio (Varian, Australia). The thickness of the films was determined by means of ellipsometry (ELX-02C, Dre Germany). Hydrophilic properties of the prepared films were estimated by measuring the contact angle of water using a CAM 100 optical contact angle meter (KSV Instruments).

Photocatalytic Testing. The photocatalytic tests were performed in an aqueous solution using methylene blue (Aldrich, λ_{max} = 661 nm) as the probe molecule. The samples were irradiated with 1 mW/cm² UV(A) light (20 W UV tube, Eurolite). The sample was preirradiated with UV(A) light (1 mW/cm²) for 24 h to decompose the remaining organic contamination by photocatalytic reaction. The TiO_2 thin films (3.5 cm × 2.5 cm) were horizontally fixed in the upper part of a cylindrically shaped glass cell with an inside diameter of 5.5 cm and a height of 6.5 cm and then immersed into the cell. The concentration of dye adsorption and test solutions was 0.02 and 0.01 mmol/L, respectively. One hundred milliliters of the MB solution was put in contact with the thin films allowing the dye to adsorb in the dark for 12 h. After the adsorption of the dye was complete, the sample was put in contact with 0.01 mmol/L MB solution and irradiated with 1 mW/cm² UV light. The photodegradation of the dye was followed by measuring the absorption spectra at regular intervals (every 20 min) using a UV/vis

10406

dx.doi.org/10.1021/jp200892z |*J. Phys. Chem. C* 2011, 115, 10405–10411

spectrophotometer Cary 100Bio (Varian, Australia). The photonic efficiency ζ being defined as the ratio of the degradation rate and the incident photon flux was calculated for all tested films from these results.

Quantitative Estimate of the Adhesion of the Prepared Films after UV Irradiation. The prepared films were irradiated for a total time of three months using a UV(A) lamp (1 mW/cm^2). The cross-cut test was applied according to the DIN EN ISO 2409 standard to obtain a qualitative impression of the adhesion of the deposited layers on the polycarbonate surface after exposure to UV irradiation. The cross-cut test was applied manually. The coated polycarbonate sheets were crisscrossed with a razor blade to form small squares (0.5 cm × 0.5 cm). An adhesive tape was stuck on the network surface and hauled almost with constant force. A part of the squared surface crumbled from the edge of the squares. These crumblings are a measure of the adhesion quality. A microscope (Olympus IXSO) was used with zoom lenses (×40). According to DIN EN ISO 2409, the quality of adhesion is ranked by different numbers ranging from 0 to 5 with the following ranking: 0 = excellent, 1 = very good, 2 = good, 3 = moderate, 4 = poor, and 5 = very poor.

■ RESULTS AND DISCUSSIONS

Characterization of the Prepared Films. The polycarbonate (PC) substrates have been first precoated by a SiO$_2$ thin film, and subsequently the precoated PC films were dipped into ethanolic
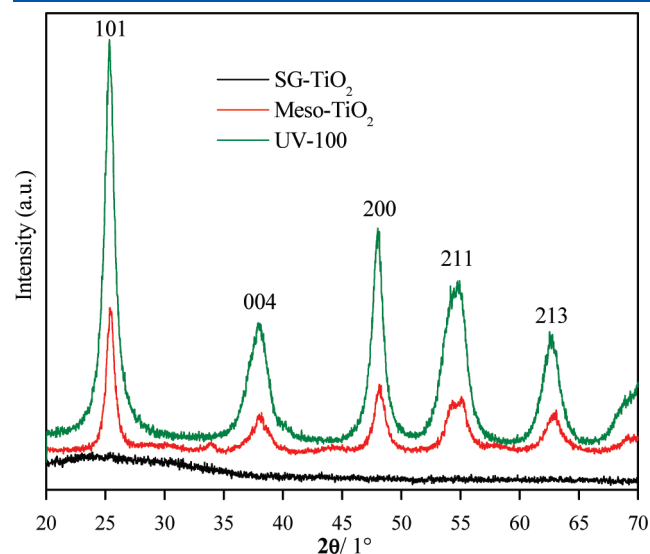
suspensions of either meso-TiO$_2$, SG-TiO$_2$, or Hombikat UV-100. The role of the SiO$_2$ layer is (i) to enhance the binding between the organic polymer PC and the inorganic TiO$_2$ layer and (ii) to protect the PC from the TiO$_2$ layer which otherwise may induce photodegradation of the PC. The X-ray diffraction patterns of SG-TiO$_2$, meso-TiO$_2$, and Hombikat UV-100 are shown in Figure 1. XRD patterns for meso-TiO$_2$ and Hombikat UV-100 show reflections with peaks characteristic for the (101), (004), (200), (211), and (213) lattice planes of the anatase phase. meso-TiO$_2$ calcined at 450 °C exhibits a three times lower crystallinity than UV-100; however, X-ray diffraction of SG-TiO$_2$ shows a very low intensity and broad bands. The TiO$_2$ crystallite sizes, indicated in Figure 1, were calculated from the width at half-maximum of the XRD reflections main peak at $2\theta = 25.2°$ employing Scherrer's equation.[22] TiO$_2$ nanocrystal sizes are 10 nm for either meso-TiO$_2$ or Hombikat UV-100, while the TiO$_2$ crystallite size in the SG-TiO$_2$ sample is <5 nm (Table 1).

Nitrogen adsorption isotherms of mesoporous TiO$_2$ and of Hombikat UV-100 are shown in Figure 2. Typical reversible type IV adsorption isotherms are found for mesoporous TiO$_2$. The sharpness of the inflection resulting from capillary condensation at relative pressures p/p_0 between 0.45 and 0.7 is characteristic for mesopores ordered in two-dimensional hexagonal symmetry. The surface areas of mesoporous TiO$_2$ and of UV-100 are 174 and 234 m^2 g^{-1}, respectively, and their pore volumes are 0.29 and 0.32 cm^3 g^{-1}, respectively. Compared with the diameter of the TiO$_2$ nanocrystallites of ~10 nm (Table 1), the wall thickness is found to be slightly smaller, implying that some of the TiO$_2$ nanocrystals could partially pierce even into the channel space.[23]
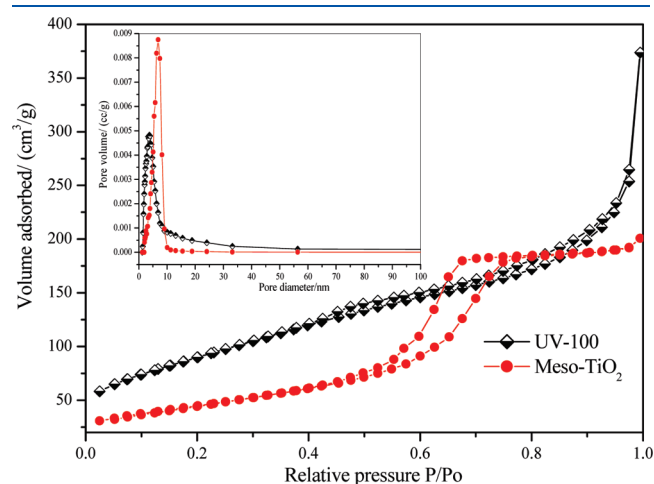

Figure 1. X-ray diffractions of mesoporous TiO$_2$, SG-TiO$_2$, and commercial Hombikat UV-100.

Figure 2. N$_2$ sorption isotherms and pore size distributions (inset) of mesoporous TiO$_2$ and of commercial Hombikat UV-100.

Table 1. Textural and Photocatalytic Properties of meso-TiO$_2$ and of Films Prepared from Commercial Sachtleben Hombikat UV100, SG-TiO$_2$, and Pilkington Activ^{TM} Photocatalysts

| photocatalyst | TiO$_2$ phase | particle size, nm | thickness, nm | contact angle | | % ζ^a |
				before UV irradiation	after UV irradiation	
UV-100	anatase	10	186 ± 19	54 ± 3	≤5	0.028
SG-TiO$_2$	anatase	5	132 ± 10	0	≤5	0.009
meso-TiO$_2$	anatase	10	203 ± 4	48 ± 5	≤5	0.078
Pilkington	anatase	—	20 ± 4	67 ± 2	≤5	0.026

^{a} % ζ: photonic efficiency for methylene blue degradation.

10407

dx.doi.org/10.1021/jp200892z |J. Phys. Chem. C 2011, 115, 10405–10411

The absence of a hysteresis loop for the commercial photocatalyst Sachtleben Hombikat UV-100 (Figure 2) shows that the mesoporosity that this sample exhibits is even less than that of *meso*-TiO$_2$; i.e., all pores can be regarded as irregular voids between TiO$_2$ particles.[20]
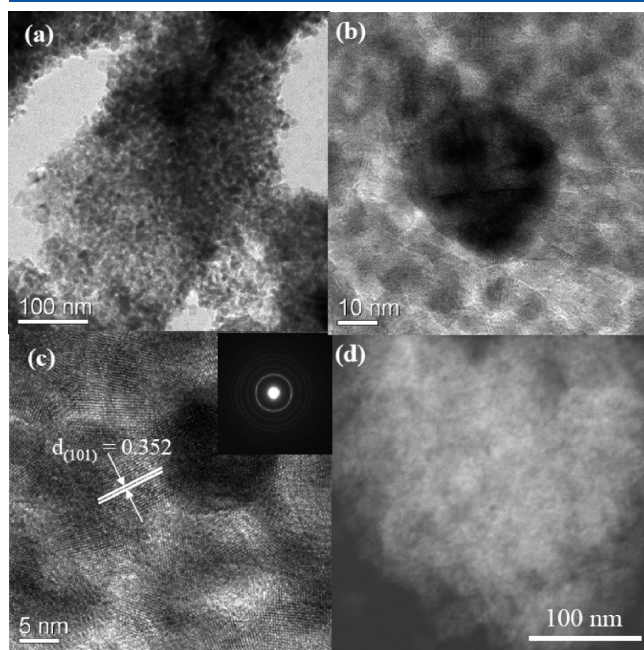
TEM images of the mesoporous TiO$_2$ and of Hombikat UV-100 are presented in Figure 3. This overview proves the exclusive presence of mesoporous TiO$_2$ nanoparticles with an average diameter of about 10 nm; the particles are not agglomerated and quite uniform in size and shape (Figure 3a). An overview image at low magnification illustrates that the self-prepared TiO$_2$ exhibits an ordered mesostructure (Figure 3b). Both the HRTEM image (Figure 3c) and the selective area electron diffraction (SAED, inset Figure 3c) show well-resolved (101) lattice fringes (distance: 0.352 nm) and diffraction cycles indicative of a highly crystalline TiO$_2$ anatase framework. The particle size of these TiO$_2$ nanocryst-
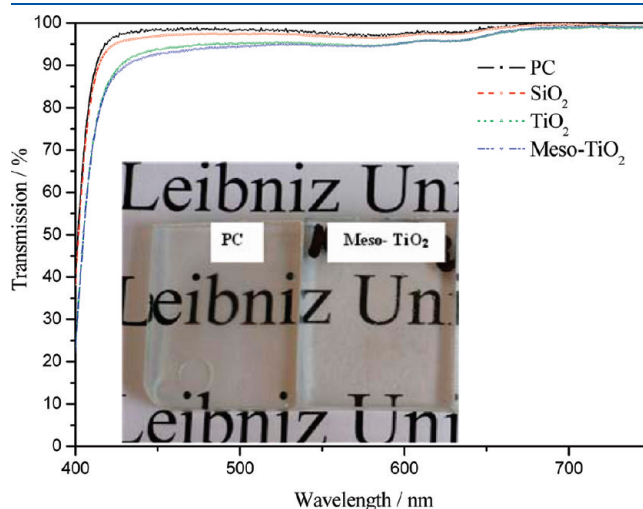

Figure 3. TEM images of mesoporous TiO$_2$ powder calcined at 450 °C (a). Overview image mesoporous TiO$_2$ at low magnification (b). HRTEM image of TiO$_2$ anatase phase using (101) (c).The inset shows the SAED patterns for the anatase phase at 450 °C (c) and the dark-field TEM image of commercial Hombikat UV-100 (d).

Figure 5. Optical transmission spectra of an uncoated polycarbonate (PC) substrate and a PC substrate precoated with SiO$_2$, SGTiO$_2$, and *meso*-TiO$_2$. Inset: the digital photograph of a PC substrate (left) and a *meso*-TiO$_2$/SiO$_2$/coating on PC substrate (right).
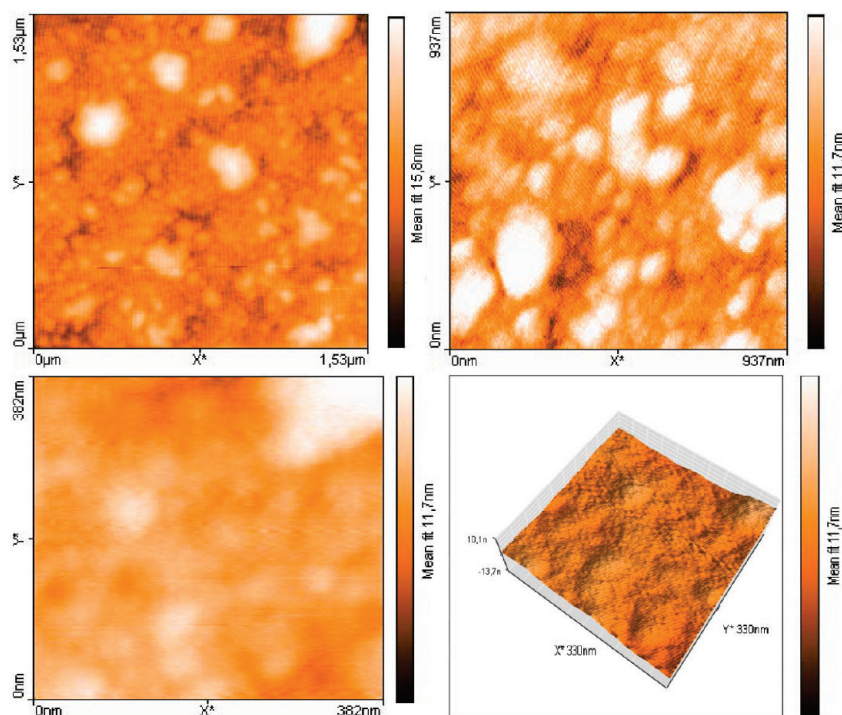

Figure 4. Two-dimensional and three-dimensional AFM image of a mesoporous TiO$_2$ film deposited onto the surface of PC substrate.
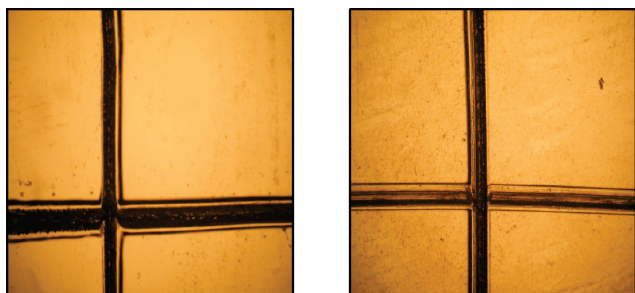
Figure 6. Images of prepared films after applying cross-cut test after three months of UV irradiation: left, TiO$_2$ (UV100); right, *meso*-TiO$_2$.

als has been measured to be between 8 and 10 nm. The dark-field TEM image of commercial Hombikat UV-100 showed that TiO$_2$ is homogeneous with its particle size being 10 nm; however, there is no clear mesoporosity even of the interparticle space (Figure 3d).

Figure 4 shows the two- and three-dimensional AFM images of the *meso*-TiO$_2$ films, clearly evincing the distribution of TiO$_2$ on PC substrate. It can clearly be seen from the height images that the nanoparticles present a relatively rough textured surface, with an rms roughness of 1.32 nm (rms represents the standard division of the values Z, with Z being the total height range analyzed).

Figure 5 shows the optical transmission spectra of a PC substrate that has been precoated with SiO$_2$ and then coated with either *meso*-TiO$_2$ or Hombikat UV-100 films. The film coatings are highly transparent, even after the formation of anatase nanocrystals, and the substrate has not been damaged. Interestingly, both *meso*-TiO$_2$ as well as the Hombikat UV-100 films showed transmittance values exceeding 95% over the entire visible wavelength range which are most likely caused by their high porosity, the small particle size, and the surface uniformity; they also meet the optical requirements for self-cleaning applications. In addition, the inset in Figure 5 shows the digital photographs of a precoated PC substrate and of a *meso*-TiO$_2$ coating. It is clearly seen that the mesoporous films prepared here are transparent and homogeneous. In turn, the thickness of the films was measured to be ∼203 ± 4 nm.

To test the stability and the adhesion quality of the thin films before and after irradiation, the adhesion quality was measured using optical microscopy (Figure 6). The thin film samples were subjected to UV radiation for three months, and then a network of small squares was applied to the surface using a sharp instrument in order to facilitate the removal of the TiO$_2$ and SiO$_2$ layers. A tape was put on the surface, and then it was removed at 60° applying a certain force. The results revealed that the prepared films are stable and adhesive. This is attributed to the formation of an intermediate layer connecting between the organic polymer and the inorganic TiO$_2$ layer.

The following mechanism is proposed to explain the above-described observations. The SiO$_2$ precoating of the PC substrates followed by the TiO$_2$ film formation enhances the acidity of the films. Subsequently, water molecules that lead to the formation of hydroxyl groups are adsorbed preferentially to the pollutant species. It is postulated that the increase in acidity is the main reason for the improved photocatalytic performance as well as for the hydrophilicity of these coatings (vide infra). The wettability of the surfaces was characterized by measuring the contact angles of films after exposure to UV light for 24 h (Table 1). In the dark, the contact angles of the samples amounted to 50−70°. For the

TiO$_2$ thin films, the UV(A) irradiation resulted in a decrease of the water-contact angle of the coated slides to zero within a few hours of UV-exposure time after which the surfaces were found to be superhydrophilic. Droplets of water spread quickly on the surface once the contact angle was <5°, which corresponds to a superhydrophilic surface (Table 1). This should lead to a considerable increase in the photonic efficiency due to the high amount of hydroxyl groups on the surface.[24] The contact angles of the prepared films were measured after three months. The prepared film stayed hydrophilic exhibiting a contact angle equal to <5°. It should be noted that good hydrophilicity should be regarded as an essential ingredient of self-cleaning technologies.

Photocatalytic Activity. Anatase TiO$_2$ is a semiconductor with a large band gap energy (E_g = 3.2 eV). Upon excitation by light of appropriate wavelength (λ < 385 nm), each of the absorbed photons can generate an electron−hole pair within the bulk or at the TiO$_2$ surface. The hole in the valence band can react with H$_2$O or hydroxide ions adsorbed at the particle surface to produce hydroxyl radicals (OH$^\bullet$), while the electron in the conduction band can reduce O$_2$ to produce superoxide radicals (O$_2^{\bullet-}$) and subsequently other reactive oxygen species (i.e., H$_2$O$_2$ and OH$^\bullet$). Both holes and OH$^\bullet$ are extremely reactive toward organic compounds with which they are in contact.[25] The photocatalytic efficiencies of the newly synthesized mesoporous TiO$_2$ films were assessed for the photodegradation of aqueous solutions of methylene blue (MB) (0.01 mmol/L) and quantitatively compared with either commercial photocatalysts (Hombikat UV100) or with Pilkington Glass Activ^{TM} by the determination of the respective photonic efficiencies. Thin films (3.5 cm × 2.5 cm) were immersed in 100 mL of MB (0.01 mmol/L) solution and irradiated with 1mW/cm^2 UV(A) light. The decomposition of the dye under UV(A) light irradiation was determined by measuring absorption spectra using a UV/vis spectrophotometer. The experimental results are shown in Figure 7. The strong absorption bands of MB located at λ = 291 nm and λ = 661 nm steadily decrease upon increasing irradiation times. This experiment clearly shows that the decoloration of MB can be achieved under UV-light irradiation when the solution is put in contact with the thin films. MB can decolorize either by the oxidative degradation of the dye or by the two-electron reduction to its colorless form.[26] We could detect a small peak of the characteristic absorption band of leuco-MB at 256 nm. Hence, the decoloration of MB is attributed to the oxidative degradation of the dye. As shown in Figure 6, the photocatalytic activity improved significantly when *meso*-TiO$_2$ was employed. The film made from ordered mesoporous TiO$_2$ shows the highest photocatalytic activity for MB decolorization. For this film, the absorbance at 664 nm decreases from 0.85 to 0.15 after nearly 24 h of irradiation. In contrast, Pilkington Glass Activ^{TM} used as a reference was only able to induce a decoloration of the MB solution to an absorbance value of 0.45 at 664 nm. The SG-TiO$_2$ thin films coated on PC exhibit even lower photocatalytic activity due to the reduced calcinations temperatures.

A correlation between the photonic efficiencies and the type of TiO$_2$ thin film employed has been clearly observed in comparison with Pilkington Glass Activ^{TM} as reference (Table 1). The photodegradation efficiency of hexagonal mesoporous TiO$_2$ exceeds that of Hombikat UV-100 thin films, although the Hombikat TiO$_2$ material is a highly crystalline anatase phase (100% anatase phase) and is, thus, much more crystalline than most of the newly prepared *meso*-TiO$_2$ films (cf. XRD diffractions results, vide supra). This difference cannot be explained by
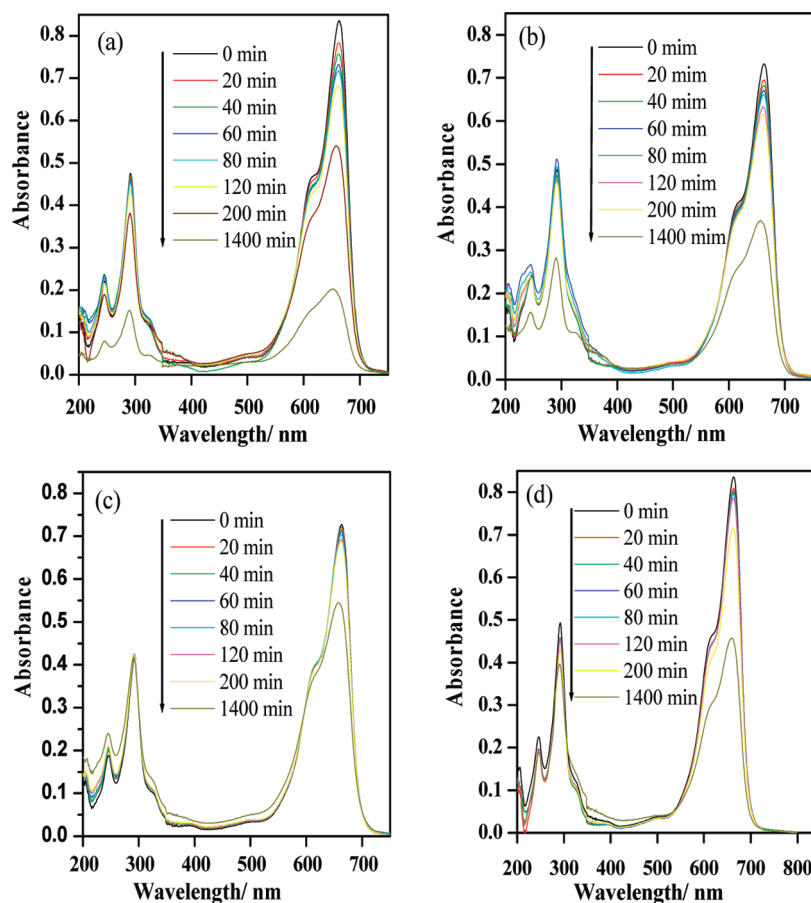
Figure 7. Absorbance vs wavelength as a function of illumination time for the photocatalytic degradation of methylene blue on thin films of *meso*-TiO$_2$ (a), commercial Hombikat UV-100 (b), SG-TiO$_2$(c), and commercial Pilkington Glass Activ^{TM} (d) (I = 1 mW/cm^2, MB concentration [0.01 mmol/L], volume of MB (test solution) = 100 mL, illuminated PC area =3.5 cm × 2.5 cm).

different surface areas or crystallinity, both of which are even higher for the Hombikat material (cf. Table 1). The high photonic efficiencies of the mesoporous TiO$_2$ film as compared with the Hombikat UV100 films can rather be attributed to different effects, such as a lower light scattering effect of the ordered mesopores, an accumulated local concentration of •OH,[27,28] and/or a fast transport of the target molecule MB to the active sites. The latter can be expected due to its facile diffusion through the ordered porous network, which for Hombikat UV-100, as well as for Pilkington Glass Activ^{TM}, is hindered by the heterogeneities existing in the bulk sample. Therefore, we conclude that the mesosporous TiO$_2$ supports the transport properties of all reactants involved in the photocatalytic process and, thus, enhances the overall photocatalytic activity. Hence, the photocatalytic •OH production is expected to occur mainly on an internal surface. Furthermore, MB adsorption onto *meso*-TiO$_2$ should take place mainly within the pores of this high surface area material. Therefore, it can be expected that the concentration of MB inside the pores will be higher in the latter samples as compared with Hombikat UV-100. Although the films prepared from *meso*-TiO$_2$ and from Hombikat UV-100 have the same thickness (∼200 nm), the photonic efficiency of *meso*-TiO$_2$ is found to be three times higher than the photonic efficiency of the Hombikat UV-100 films. This is attributed to the photonic efficiency being limited by the diffusion rate of the MB molecule to the photocatalytically active surface, as a result of the

difference in the size and the number of pores. The results revealed that the *meso*-TiO$_2$ photocatalyst film was quite stable and adhesive, thus showing a good potential for self-cleaning applications.

■ **CONCLUSIONS**

In summary, a new strategy has been developed for the preparation of TiO$_2$ thin films for self-cleaning applications. Highly crystalline, mesoporous TiO$_2$ films have been deposited on a PC substrate using a dip-coating process. The photodegradation of methylene blue showed that meso-ordered TiO$_2$ has a three times higher photocatalytic activity than films prepared from commercial Hombikat UV100 and Pilkington Glass Activ^{TM}, respectively. The improved efficiency and potentially the low-cost synthesis suggest that this material might be practically useful as a photocatalyst film. This effect is mainly attributed to a closer contact between MB molecules and the TiO$_2$ surface resulting in an improved diffusion in the porous network of the mesoporous TiO$_2$. By making use of the characteristics of the *meso*-TiO$_2$ thin film, this work opens the way to a more extended investigation employing polycarbonate for self-cleaning applications. The newly synthesized transparent *meso*-TiO$_2$ thin films have the potential to considerably reduce the price barrier and to open up new production technologies for low-cost self-cleaning applications.

■ AUTHOR INFORMATION

Corresponding Author
*E-mail: aismail@cmrdi.sci.eg

■ ACKNOWLEDGMENT

■ REFERENCES

(1) Subedi, D. P.; Zajickova, L.; Bursikova, V.; Janca, J. *Himalayan J. Sci.* **2003**, *1*, 115–118.

(2) Wang, T.; Wang, H.; Xu, P.; Zhao, X. C.; Chao, S. *Thin Solid Films* **1998**, *334*, 10.

(3) Sheng, J.; Shivalingappa, L.; Karasawa, J.; Fukami, T. *J. Mater. Sci.* **1999**, *34*, 6201.

(4) Bao, X. W.; Zhang, J. L. *Acta Phys. Chim. Sin.* **2005**, *21*, 69.

(5) Langlet, M.; Burgos, M.; Coutier, C.; Jimenez, C.; Morant, C.; Manso, M. *J. Sol−Gel Sci. Technol.* **2001**, *22*, 139.

(6) Dutschke, A.; Diegelmann, C.; Lobmann, P. *J. Mater. Chem.* **2003**, *13*, 1058.

(7) Kwon, C. H.; Shin, H.; Kim, J. H.; Choi, W. S.; Yoon, K. H. *Mater. Chem. Phys.* **2004**, *86*, 78.

(8) Zhou, L.; Yan, S.; Tian, B.; Zhang, J.; Anpo, M. *Mater. Lett.* **2006**, *60*, 396–399.

(9) Mao, Y.; Schoneich, C.; Asmus, K. D. Radical Mediated Degradation Mechanisms of Halogenated Organic Compounds As Studied by Photocatalysis at TiO_2 and by Radiation Chemistry. In *Photocatalytic Purification of Water and Air*; Ollis, D. E., Al-Ekabi. H., Eds.; Elsevier: New York, 1993; pp , 49−66.

(10) Ismail, A. A.; Bahnemann, D. W.; Bannat, I.; Wark, M. *J. Phys. Chem. C* **2009**, *113*, 7429–7435.

(11) Ohko, Y.; Tryk, D. A.; Hashimoto, K.; Fujishima, A. *J. Phys. Chem. B* **1998**, *102*, 2699.

(12) Anpo, M.; Shima, T.; Kodama, S.; Kubokawa, Y. *J. Phys. Chem.* **1987**, *91*, 4305.

(13) Kato, K.; Tsuzuki, A.; Taoda, H.; Torii, Y.; Kato, T.; Butsugan, Y. *J. Mater. Sci.* **1994**, *29*, 5911.

(14) Imai, H.; Morimoto, H.; Tominaga, A.; Hirashima, H. *J. Sol−Gel Sci. Technol.* **1997**, *10*, 45–54.

(15) Wang, R.; Hashimoto, K.; Fujishima, A.; Chikuni, M.; Kojima, E.; Kitamura, A.; Shimohigoshi, M.; Watanabe, T. *Nature (London)* **1997**, *388*, 431.

(16) Mark, D. E. *Nature* **2002**, *417*, 813–821.

(17) Maldotti, A.; Molinari, A.; Amadelli, R.; Carbonell, E.; Garcia, H. *Photochem. Photobiol. Sci.* **2008**, *7*, 819.

(18) Alvaro, M.; Aprile, C.; Benitez, M.; Carbonell, E.; Garcia, H. *J. Phys. Chem. B* **2006**, *110*, 6661–6665.

(19) Kumar, K. P. *Appl. Catal., A* **1994**, *119*, 163–83.

(20) Ismail, A. A.; Bahnemann, D. W.; Robben, L.; Yarovyi, V.; Wark, M. *Chem. Mater.* **2010**, *22*, 108.

(21) Gregg, S. J.; Sing, K. S. W. *Adsorption, surface area, and porosity*; Academic Press: London, 1982.

(22) Azároff, L. V.; Buerger, M. J. *The powder method in x-ray crystallography*; McGraw-Hill: New York, 1958; p 255.

(23) Liu, R.; Ren, Y.; Shi, Y.; Zhang, F.; Zhang, L.; Tu, B.; Zhao, D. *Chem. Mater.* **2008**, *20*, 1140–1146.

(24) Feng, X.; Zhai, J.; Jiang, L. *Angew. Chem., Int. Ed.* **2005**, *44*, 5115.

(25) Hoffmann, M. R.; Martin, S. T; Choi, W.; Bahnemann, D. W. *Chem. Rev.* **1995**, *95*, 69.

(26) Park, H.; Choi, W. *J. Phys. Chem. B* **2005**, *109*, 11667.

(27) Lawless, D.; Serpone, N.; Meisel, D. *J. Phys. Chem.* **1991**, *95*, 5166–5170.

(28) Tojo, S.; Tachikawa, T.; Fujitsuka, M.; Majim, T. *Chem. Phys. Lett.* **2004**, *384*, 312–316.